

Research on Dynamics of MCCB Operating Mechanism based on Singular Configurations

Wang Jun¹ Hang Lubin*¹ Huang Xiaobo¹ Xiang Honggang² Yu Yipeng²

¹College Of Mechanical Engineering, Shanghai University Of Engineering Science, Shanghai 201600;

²Shanghai Liangxin Electrical Co. , Ltd. , Shanghai 200137)

Abstract: The design of operating mechanism of Molded Case Circuit Breaker (MCCB) should ensure various targets of the performance. However, the coupling of various performance, indexes and structure parameters results in difficulty of the design and optimization of operating mechanism. Based on the singular configurations of MCCB operating mechanism, the closing process is divided into three motion phases to study the different structure in different phase. Lagrange dynamics equations are built and the characteristics of the first and second singular configuration are studied. The closing operation velocity curve of the operating mechanism is simulated in ADAMS. It provides theoretical basis for the analysis of the MCCB performance.

Keywords: MCCB; operating mechanism; the first singular configuration; the second singular configuration; Lagrange dynamics equations

I. INTRODUCTION

With the development of smart grid, molded case circuit breakers (MCCBs) are required to achieve the following performance: 1) high breaking capacity; 2) high reliability; 3) high consistency [1,2]. As the core component of MCCB, operating mechanism plays an important role in the closing operation.

Degui Chen built a novel dynamic model of MCCB's operating mechanism based on multi-body dynamics adopting virtual prototyping technology, and made an experiment to verify the mechanical properties of MCCB. Based on that, the effect of different factors to the operating velocities of mechanism was analyzed [3,4]. A process model of MCCB operating characteristic multidimensional analysis and a dynamic model were established by Hongming Zhou. Based on Lagrange equations, design parameters of operating mechanism including breaking velocity, opening range, spring force were analyzed and optimized by simulation in ADAMS [5,6].

These existing papers focus on the movement process and kinematic properties for MCCB operating mechanisms using virtual prototyping technology in ADAMS, but literature on the singular configurations of the operating mechanism is limited. As a special position during the MCCB closing operation, the second singular configuration is important to the design of an operating mechanism.

The paper introduces the notion of the first singular configuration and the second singular configuration of MCCB operating mechanism. Based on the singular configurations, the closing process is divided into three motion phases and the different structure in different phase is studied. Dynamic model and static dynamics model are built to study connection between the first and second singular configuration. And in ADAMS, the closing operation velocity curve of the operating mechanism is simulated.

*Corresponding author. E-mail address:
hanglb@126.com

II. STRUCTURE AND MOTION PHASES OF OPERATING MECHANISM

2.1 Structure

A simplified version of the operating mechanism of a MCCB (Fig. 1a) is shown in Fig. 1b. Here, the handle K and crank D are pivoted to the ground at 'K' and 'F' respectively. The crank of a four-bar chain is connected to the handle via the main spring G which is an interconnected tension spring. S1, S2, S3, and S4 are the four stoppers, determining the desired end states for the handle and crank respectively. User input to the handle is

transferred to the crank through the main spring, then the crank drives the moving link AB making contact with the fixed contact during a closing process of a MCCB.

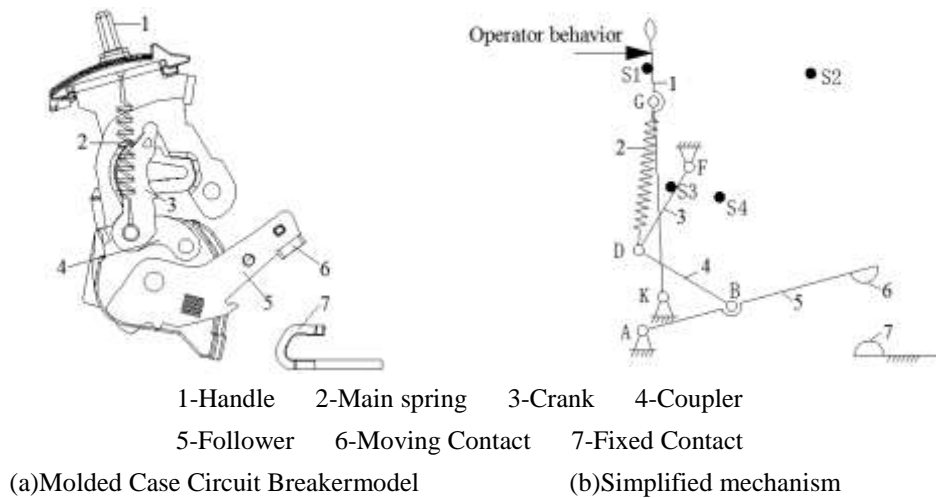


Fig. 1. A Molded Case Circuit Breaker mechanism

2.2 Motion Phases Based on the Singular Configuration

2.2.1 The first and the second singular configuration

The most of mechanisms may perform special configuration in the motion process. At configuration, the system cannot continue to move in dead center, or loses stability, even changes its degrees of freedom. The configuration is then at a branch point and is referred to as a singular configuration [7].

The transient phenomenon of closing process happens through the sequential activation of the two links, the handle and crank. The bifurcation configuration for the crank is the collinearity of the points G, F and D (Fig. 2a), which is called the first singular configuration, noted as T1. The vector-loop diagram of spring four-bar chain consisting of the handle, crank and the main spring is shown in Fig. 2b.

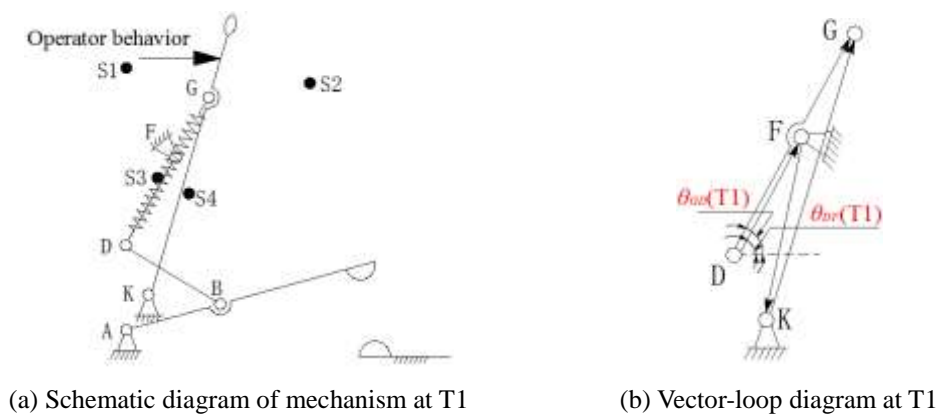


Fig. 2. The first singular configuration of operating mechanism

From Fig. 2 b, the following geometric equation of the first singular configuration can be derived:

$$\theta_{DF}(T1) = \theta_{GD}(T1) \tag{1}$$

Where $\theta_{DF}(T1)$ and $\theta_{GD}(T1)$ are the angular displacements of the main spring GD and crank DF at the first singular configuration respectively.

Similarly the collinearity of the points G, D and K defines the bifurcation configuration for the handle (Fig. 3a). This is the second singular configuration, noted as T2. The vector-loop diagram of spring four-bar chain is shown in Fig. 3b.

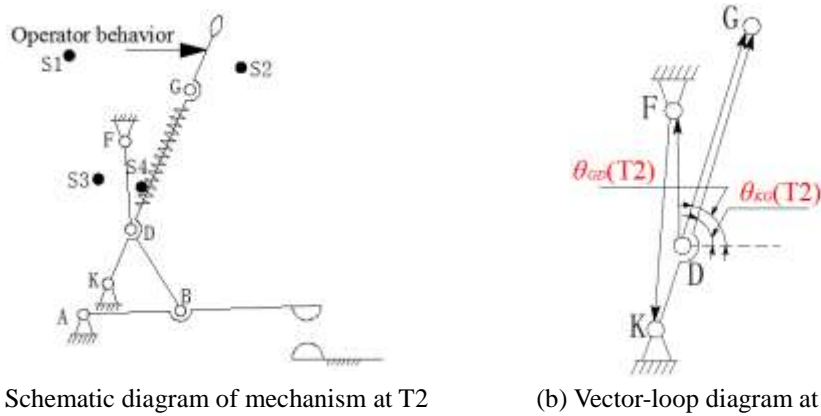


Fig. 3. The second singular configuration of operating mechanism

From Fig. 3b, the following geometric equation of the second singular configuration can be derived:

$$\theta_{KG}(T2) = \theta_{GD}(T2) \tag{2}$$

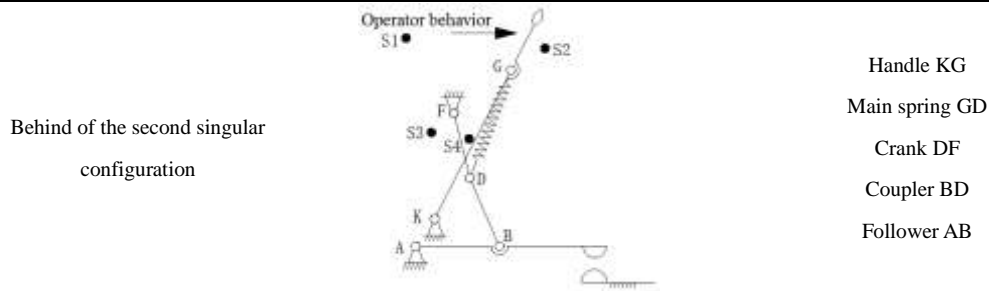
Where $\theta_{KG}(T2)$ and $\theta_{GD}(T2)$ are the angular displacements of the handle KG and main spring GD at the second singular configuration respectively.

2.2.2 Motion Phases

A MCCB mechanism has the capability to change configuration from one kind to another with a resultant change in the directions of moment due to driving forces and the number of effective links when it passes through two singular configurations during the closing process. So it can take the first and second singular configuration as the boundary conditions to divide the closing motion into three phases. Table 1 shows different phases and effective links of motion of a MCCB mechanism.

Table 1 Different phases and effective links of motion of a MCCB mechanism

Phases	Schematic diagram	effective links
Ahead of the first singular configuration		Handle KG Main spring GD (Due to the stoppers, other links stay static)
Between the first and second singular configuration		Handle KG Main spring GD Crank DF Coupler BD Follower AB



III. CHARACTERISTICS OF THE SINGULAR CONFIGURATIONS

3.1 The first singular configuration

In the case of a tension main spring, the stored potential energy is a monotonic function of its length. Actually, the spring energy reaches the local maximum when G–F–D becomes collinear which is the first singular configuration. Therefore, the internal force exerted by the spring GD attains a maximum value; also there is a maximum angle between the spring force and the handle. It can be obtained that there is the requirement of the maximum driving torque at the first singular configuration, and if a MCCB operating mechanism can reach the position of the second singular configuration, the input force must be able to overcome the spring force to cause the operating mechanism pass through the first singular configuration.

Let us make a static analysis of the handle without concerning friction at the first singular configuration. In the Fig. 4, the user-input force and the handle's gravity all create a clockwise torque in the handle, which overcoming an anti-clockwise torque in the handle produced by the spring force make the handle rotate in the clockwise direction.

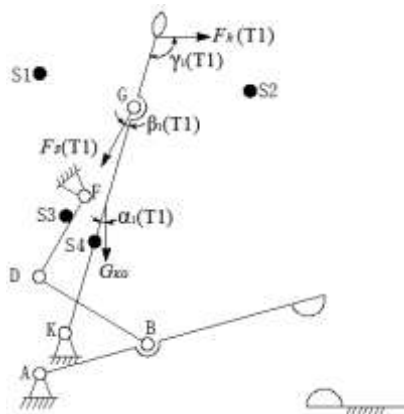


Fig. 4. Force analysis of the handle at T1

From the Fig. 4, the following statics equation (3) can be derived:

$$F_h(T1) \cdot L_{Fh} \cdot \sin \gamma_1(T1) + \frac{1}{2} \cdot G_{KG} \cdot L_{KG} \cdot \sin \alpha_1(T1) = F_s(T1) \cdot L_{KG} \cdot \sin \beta_1(T1) \quad (3)$$

where

$$\alpha_1(T1) = \frac{\pi}{2} - \theta_{KG}(T1), \quad \beta_1(T1) = \theta_{KG}(T1) - \theta_{GD}(T1), \quad \gamma_1(T1) = \pi - \theta_{KG}(T1)$$

Equation (3) can be recast to obtain the input force in the handle, $F_h(T1)$, which can make operating mechanism pass through the first singular configuration, i.e. connection between the first and second singular configuration.

$$F_h(T1) > \frac{F_s(T1) \cdot L_{KG} \cdot \sin \beta_1(T1) - \frac{1}{2} \cdot G_{KG} \cdot L_{KG} \cdot \sin \alpha_1(T1)}{L_{F_h} \cdot \sin \gamma_1(T1)} \quad (4)$$

where L_{KG} is the length of handle, L_{F_h} is the arm of user-input force.

3.2 The second singular configuration

In dynamics, the Lagrange equation is commonly used to derive the equations of motion of a MCCB operating mechanism:

$$\frac{d}{dt} \left(\frac{\partial E_k}{\partial \dot{q}_i} \right) - \frac{\partial E_k}{\partial q_i} + \frac{\partial E_p}{\partial q_i} = Q_i \quad (5)$$

where q_i is generalized coordinates and Q_i is generalized forces, E_k and E_p are total kinetic energy and the total potential energy respectively. Fig. 5 shows the schematic diagram of the operating mechanism under dynamic analysis.

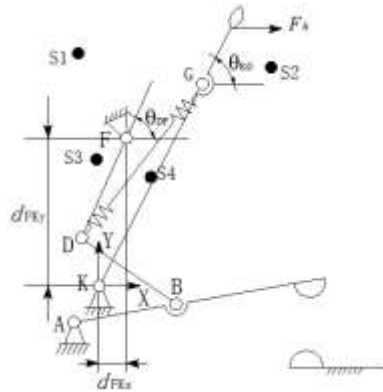


Fig. 5. Schematic diagram of dynamic analysis during closing process

Therefore, to use the Lagrange equation for deriving the motion equations of a MCCB operating mechanism, its total kinetic and potential energies must first be formulated. The procedure for the energy derivation is shown as follows [8].

The vector-loop equations can be expressed:

$$r_1 + r_2 + r_3 + \dots + r_j = 0 \quad (6)$$

By expressing equation (6) into X and Y scalar component equations and rearranging, the resultant two equations are:

$$r_1 \cos \theta_1 + r_2 \cos \theta_2 + r_3 \cos \theta_3 + \dots + r_j \cos \theta_j = 0 \quad (7)$$

$$r_1 \sin \theta_1 + r_2 \sin \theta_2 + r_3 \sin \theta_3 + \dots + r_j \sin \theta_j = 0 \quad (8)$$

During the closing operation, the handle angular displacement θ_{KG} is defined as the generalized coordinate q_1 and the crank angular displacement θ_{DF} as the generalized coordinate q_2 . Taking the crank as the equivalent rod, the equivalent mass and equivalent moment of inertia of the rigid four-bar chain ABDF is m_e and J_e respectively [9]. Hence, the total kinetic energy, E_k , in the system is obtained as

$$E_k = \frac{1}{2} \cdot m_{KG} \cdot v_{KG}^2 + \frac{1}{2} J_{KG} \cdot \dot{\theta}_{KG}^2 + \frac{1}{2} \cdot m_e \cdot v_{DF}^2 + \frac{1}{2} \cdot J_e \cdot \dot{\theta}_{DF}^2 \quad (9)$$

Assuming that the potential energy is zero at the origin of the coordinate system, the total potential energy, E_p , in the operating mechanism can be expressed as

$$E_p = m_{KG} \cdot g \cdot \frac{L_{KG}}{2} \cdot \sin\theta_{KG} + m_e \cdot g \cdot \left(d_{FKy} - \frac{L_{DF}}{2} \cdot \sin\theta_{DF} \right) + \frac{1}{2} \cdot k \cdot \Delta L_S^2 \quad (10)$$

Here, the relationship among the spring length L_S , the handle angular displacement θ_{KG} and the crank angular displacement θ_{DF} is as follows

$$\Delta L_S + L_{S0} = \sqrt{(d_{FKx} - L_{DF} \cdot \cos\theta_{DF} - L_{KG} \cdot \cos\theta_{KG})^2 + (d_{FKy} - L_{DF} \cdot \sin\theta_{DF} - L_{KG} \cdot \sin\theta_{KG})^2} \quad (11)$$

where J_{KG} is the moment of inertia of the handle KG, L_{S0} and ΔL_S are the original length and increase length of the spring respectively, k is the stiffness of the spring, d_{FKx} and d_{FKy} are the horizontal and vertical distance between the fixed point F and K respectively.

When the total kinetic and potential energies are substituted into the Lagrange equation, the dynamic equations can be expressed as follows

$$\left(\frac{d}{dt} \left(\frac{\partial E_k}{\partial \dot{\theta}_{KG}} \right) - \frac{\partial E_k}{\partial \theta_{KG}} + \frac{\partial E_p}{\partial \theta_{KG}} \right) = M(F) \quad (12)$$

$$\left(\frac{d}{dt} \left(\frac{\partial E_k}{\partial \dot{\theta}_{DF}} \right) - \frac{\partial E_k}{\partial \theta_{DF}} + \frac{\partial E_p}{\partial \theta_{DF}} \right) = 0 \quad (13)$$

Where

$$\begin{aligned} \frac{d}{dt} \left(\frac{\partial E_k}{\partial \dot{\theta}_{KG}} \right) &= \frac{1}{4} \cdot (m_{KG} \cdot L_{KG}^2 + J_{KG}) \cdot \ddot{\theta}_{KG} + \left(\frac{1}{4} \cdot m_e \cdot L_{DF}^2 + J_e \right) \cdot \frac{\partial \dot{\theta}_{DF}}{\partial \dot{\theta}_{KG}} \cdot \ddot{\theta}_{DF} \\ &+ \left[\frac{\partial \dot{\theta}_{DF}}{\partial \dot{\theta}_{KG}} \cdot \left(\frac{1}{4} \cdot \frac{dm_e}{dt} \cdot L_{DF}^2 + \frac{dJ_e}{dt} \right) + \left(\frac{1}{4} \cdot m_e \cdot L_{DF}^2 + J_e \right) \cdot \frac{d}{dt} \left(\frac{\partial \dot{\theta}_{DF}}{\partial \dot{\theta}_{KG}} \right) \right] \cdot \dot{\theta}_{DF} \\ &+ \frac{1}{2} \cdot \left[\frac{1}{4} \cdot \frac{d}{dt} \left(\frac{\partial m_e}{\partial \dot{\theta}_{KG}} \right) \cdot L_{DF}^2 + \frac{d}{dt} \left(\frac{\partial J_e}{\partial \dot{\theta}_{KG}} \right) \right] \dot{\theta}_{DF}^2 + \left(\frac{1}{4} \cdot \frac{\partial m_e}{\partial \dot{\theta}_{KG}} \cdot L_{DF}^2 + \frac{\partial J_e}{\partial \dot{\theta}_{KG}} \right) \cdot \dot{\theta}_{DF} \cdot \ddot{\theta}_{DF} \\ \frac{\partial E_k}{\partial \theta_{KG}} &= \left(\frac{1}{4} \cdot m_e \cdot L_{DF}^2 + J_e \right) \cdot \frac{\partial \dot{\theta}_{DF}}{\partial \theta_{KG}} \cdot \dot{\theta}_{DF} + \frac{1}{2} \cdot \left[\frac{1}{4} \cdot \left(\frac{\partial m_e}{\partial \theta_{KG}} \right) \cdot L_{DF}^2 + \left(\frac{\partial J_e}{\partial \theta_{KG}} \right) \right] \dot{\theta}_{DF}^2 \\ \frac{\partial E_p}{\partial \theta_{KG}} &= \frac{1}{2} \cdot m_{KG} \cdot g \cdot L_{KG} \cdot \cos\theta_{KG} - \frac{1}{2} \cdot m_e \cdot g \cdot L_{DF} \cdot \cos\theta_{DF} \cdot \frac{\partial \theta_{DF}}{\partial \theta_{KG}} \\ &+ \frac{\partial m_e}{\partial \theta_{KG}} \cdot g \cdot \left(d_{FKy} - \frac{1}{2} \cdot L_{DF} \cdot \sin\theta_{DF} \right) + k \cdot \Delta L_S \cdot \frac{\partial \Delta L_S}{\partial \theta_{KG}} \\ \frac{d}{dt} \left(\frac{\partial E_k}{\partial \dot{\theta}_{DF}} \right) &= \left(\frac{1}{4} \cdot m_{KG} \cdot L_{KG}^2 + J_{KG} \right) \cdot \left[\frac{\partial \dot{\theta}_{KG}}{\partial \dot{\theta}_{DF}} \cdot \ddot{\theta}_{KG} + \frac{d}{dt} \left(\frac{\partial \dot{\theta}_{KG}}{\partial \dot{\theta}_{DF}} \right) \cdot \dot{\theta}_{KG} \right] + \left(\frac{1}{4} \cdot m_e \cdot L_{DF}^2 + J_e \right) \\ &\cdot \ddot{\theta}_{DF} \\ &+ \left(\frac{1}{4} \cdot \frac{dm_e}{dt} \cdot L_{DF}^2 + \frac{dJ_e}{dt} \right) \cdot \dot{\theta}_{DF} + \left(\frac{1}{4} \cdot \frac{\partial m_e}{\partial \dot{\theta}_{DF}} \cdot L_{DF}^2 + \frac{\partial J_e}{\partial \dot{\theta}_{DF}} \right) \cdot \dot{\theta}_{DF} \cdot \ddot{\theta}_{DF} \\ &+ \frac{1}{2} \cdot \left[\frac{1}{4} \cdot \frac{d}{dt} \left(\frac{\partial m_e}{\partial \dot{\theta}_{DF}} \right) \cdot L_{DF}^2 + \frac{d}{dt} \left(\frac{\partial J_e}{\partial \dot{\theta}_{DF}} \right) \right] \dot{\theta}_{DF}^2 \\ \frac{\partial E_k}{\partial \theta_{DF}} &= \left(\frac{1}{4} \cdot m_{KG} \cdot L_{KG}^2 + J_{KG} \right) \cdot \frac{\partial \dot{\theta}_{KG}}{\partial \theta_{DF}} \cdot \dot{\theta}_{KG} + \frac{1}{2} \cdot \left[\frac{1}{4} \cdot \left(\frac{\partial m_e}{\partial \theta_{DF}} \right) \cdot L_{DF}^2 + \left(\frac{\partial J_e}{\partial \theta_{DF}} \right) \right] \dot{\theta}_{DF}^2 \\ \frac{\partial E_p}{\partial \theta_{DF}} &= \frac{1}{2} \cdot m_{KG} \cdot g \cdot L_{KG} \cdot \cos\theta_{KG} \cdot \frac{\partial \theta_{KG}}{\partial \theta_{DF}} + \frac{\partial m_e}{\partial \theta_{DF}} \cdot g \cdot \left(d_{FKy} - \frac{1}{2} \cdot L_{DF} \cdot \sin\theta_{DF} \right) \\ &- \frac{1}{2} \cdot m_e \cdot g \cdot L_{DF} \cdot \cos\theta_{DF} + k \cdot \Delta L_S \cdot \frac{\partial \Delta L_S}{\partial \theta_{DF}} \end{aligned}$$

where $M(F_h)$ is the torque of input force on the handle.

Based on the dynamic model of the operating mechanism, the simplified simulation model of the MCCB's

operating mechanism is established in ADAMS software.

IV. SIMULATION IN ADAMS

In the case of a simulation, the manual operation is represented by a pushing rod on the handle to drive the operating mechanism. Through changing the velocities of the pushing rod, hence the position of the second singular configuration under the different operator behavior velocities can be obtained. A simplified simulation model in ADAMS is shown in Fig. 6:

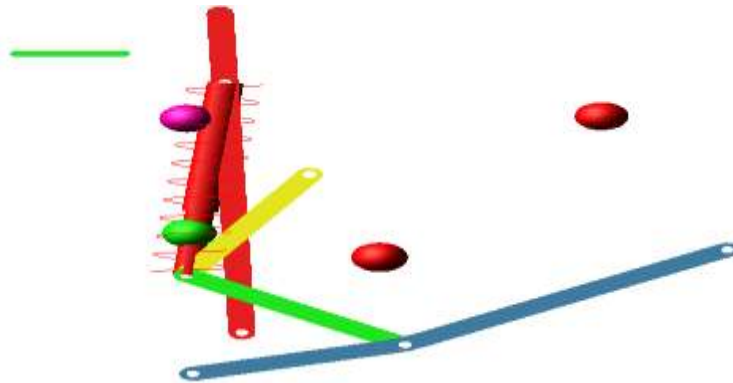


Fig. 6. Simulation of MCCB operating mechanism

Through simulation in ADAMS, the result of the angular displacement θ_{KG} with respect to the angular velocity $\dot{\theta}_{KG}$ is shown in Fig. 7:

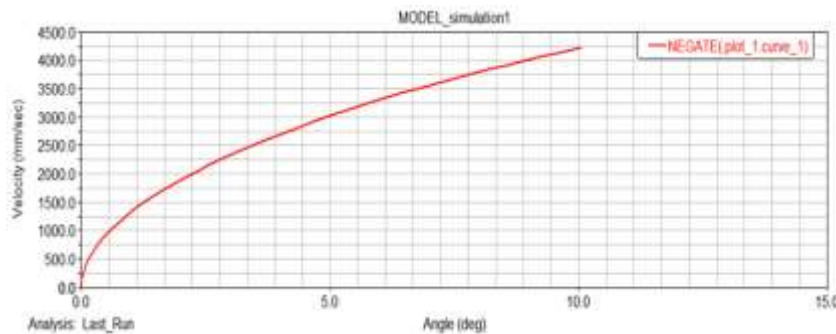


Fig. 7 The result curve of θ_{KG} with respect to $\dot{\theta}_{KG}$

CONCLUSION AND DISCUSSION

The contributions of the study aiming at the design and optimization of MCCB operating mechanisms are summarized as follows:

- 1) Based on the singular configurations, the closing process is divided into three motion phases to study the different structure in different phase;
- 2) Based on Lagrange dynamics equations, dynamic model and static dynamics mode are built to study connection between the first and second singular configuration, and the necessary condition of passing through the second singular configuration is proposed by static analysis.
- 3) The analysis and simulation provide theoretical basis for the analysis of the MCCB performance.

ACKNOWLEDGMENT

The authors would like to acknowledge the financial support of the Shanghai Committee of Science and Technology Key Support Project under Grant 12510501100 and school-enterprise cooperation project E4-6000-15-0225- (15)JX-015.

REFERENCES

- [1]. He Ruihua. The State of Low-voltage Circuit Breaker in China and Its Development Trend [J]. *Electrical Engineering*, 2009, (6): 9-13.
- [2]. Chen Degui. Smart Grid and Recent Development of Intelligent Low Voltage Electrical Apparatus [J]. *Low Voltage Apparatus*, 2010, (5): 1-6, 48.
- [3]. Zhang Jingshu, Chen Degui, Liu Hongwu. DYNAMIC SIMULATION AND OPTIMUM DESIGN OF LOW-VOLTAGE CIRCUIT BREAKER [J]. *Proceedings of the CSEE*, 2004, 24(33): 102-107.
- [4]. Chen Degui, Liu Qingjiang, Kang yan. Effect of Different Factors to the Operating Velocity of Molded Case Circuit Breakers [J]. *Low Voltage Apparatus*, 2005, (12): 9-12.
- [5]. Zhou Hongming, Shen yan, Huang shenquan, et al. Dynamic model of molded case circuit breaker operating mechanism and its performance analysis [J]. *Computer Integrated Manufacturing Systems*, 2015, 21(5): 1350-1358.
- [6]. Huang shenquan, Zhou Hongming, Zhou Yuqing, et al. Evaluation of low-voltage circuit breaker virtual prototype operating characteristic based on extension analysis [J]. *Computer Integrated Manufacturing Systems*, 2015, 21(1): 217-225.
- [7]. Huang zhen, Zhao Yongsheng, Zhao Tieshi. *Advanced Spatial Mechanism (Second Edition)* [M]. Beijing: Higher Education Press, 2014: 255-284.
- [8]. F-C Chen, Y-F Tzeng. On the dynamics of a spring-type operating mechanism for a gas-insulated circuit breaker in open operation using the Lagrange equation [J]. *Proceedings of the Institution of Mechanical Engineers*, 2002, 216(C8): 831-843.
- [9]. Ye Xinquan, Zhao Rongxiang, Wu Maogang. Study on breaking action characteristics of moulded case circuit-breaker contact [J]. *Journal of Zhejiang University(Engineering Science)*, 2006, 40(3): 448-453.